J. Fluid Mech. (1991), *vol.* 229, *pp.* 135–158
Printed in Great Britain

Evolution of weakly nonlinear water waves in the presence of viscosity and surfactant

By S. W. JOO[1]†, A. F. MESSITER[2] AND W. W. SCHULTZ[1]

[1] Department of Mechanical Engineering and Applied Mechanics, University of Michigan, Ann Arbor, MI 48109–2125, USA

[2] Department of Aerospace Engineering, University of Michigan, Ann Arbor, MI 48109, USA

(Received 21 August 1989 and in revised form 23 January 1991)

A formal derivation of evolution equations is given for viscous gravity waves and viscous capillary–gravity waves with surfactants in water of infinite depth. Multiple scales are used to describe the slow modulation of a wave packet, and matched asymptotic expansions are introduced to represent the viscous boundary layer at the free surface. The resulting dissipative nonlinear Schrödinger equations show that the largest terms in the damping coefficients are unaltered from previous linear results up to third order in the amplitude expansions. The modulational instability of infinite wavetrains of small but finite amplitude is studied numerically. The results show the effect of viscosity and surfactants on the Benjamin–Feir instability and subsequent nonlinear evolution. In an inviscid limit for capillary–gravity waves, a small-amplitude recurrence is observed that is not directly related to the Benjamin–Feir instability.

1. Introduction

Although water waves are usually described adequately by inviscid-flow theory, the effects of viscosity and interfacial properties become important for waves of short wavelength. For sufficiently short waves, the shear-stress boundary condition, which is neglected in classical studies, must then be satisfied at the free surface. If the free surface is clean and the air above is ignored, the shear-stress vanishes. However, when a layer of contaminant (surfactant) is present on the free surface, its concentration varies with the motion of the free surface, causing a surface-tension gradient that must be balanced by a non-zero surface shear stress. Studying waves of short wavelength is important in radar remote sensing of the sea surface, and surfactants affect these remote images strongly.

The highly dissipative effect of surfactants has been observed since classical times (Pliny, 77 AD). A qualitative explanation of dissipation caused by variations in surface tension was given by Reynolds (1880), as cited by Lamb (1932). Levich (1941, 1962) later performed a more thorough analysis, and an extension of this work was described in the review by Lucassen-Reynders & Lucassen (1969). Miles (1967) has described surface-wave damping in closed basins, including the effects of a surfactant as well as of solid boundaries. In these mathematical models the surfactant was considered as an interfacial film of infinitesimal thickness, with surface tension determined by surfactant concentration. A series of more complicated models

† Current address: Department of Engineering Sciences and Applied Mathematics, Northwestern University, Evanston, IL 60208, USA.

proposed by Goodrich (1960, 1962) treated the surfactant as an anisotropic rheological body. A simpler viscoelastic interfacial constitutive equation that compared favourably with experimental measurements was developed by Addison & Schechter (1979). Extensive references describing the various effects of surfactants on water waves are given by Lucassen (1982).

In the aforementioned investigations, the study of viscous damping associated with water waves has been confined to linear theory, in which the wave amplitude is infinitesimal and the free-surface boundary conditions are applied at a mean surface. For weakly nonlinear waves without damping, the slow amplitude evolution is described by the nonlinear Schrödinger equation (NLS), first introduced for water waves by Zakharov (1968) with a variational method and obtained by Hasimoto & Ono (1972) using a multivariable method. Comprehensive discussions and extensive references for the nonlinear dynamics of deep-water gravity waves were given in the reviews by Yuen & Lake (1980, 1982) and in the book by Mei (1983). An extension to capillary–gravity waves was given by Djordjevic & Redekopp (1977).

The damping effect has sometimes been included in the analysis of deep-water gravity waves through the addition of conjectured small dissipation terms in the NLS equation. While a generally accepted model uses a linear dissipation term, Lake *et al.* (1977) and Pereira & Stenflo (1977) included nonlinear representations. Miles (1988) considered weakly nonlinear, weakly damped, deep-water capillary–gravity waves, and allowed the possibility of a contaminated surface. The NLS equation, augmented by a linear damping term, was obtained with the known values of the damping coefficient stated for a clean surface or for an inextensible contaminated surface.

The present work develops amplitude equations using matched asymptotic expansions as well as multiple scales, since both boundary-layer and potential-flow solutions are required. Flow details are shown for specific choices concerning the relative orders of magnitude of three small parameters representing non-dimensional amplitude, viscosity and surface-tension variation. Non-diffusive insoluble surfactants are considered, and the surface-tension changes are represented in terms of surfactant-concentration gradients. A dissipative nonlinear Schrödinger equation is obtained, and in this respect the derivation is an elaboration of the work of Miles (1988). An expression for the damping coefficient is given, higher-harmonic resonances are noted, a modification for pure capillary waves is shown, and some numerical results are obtained.

We first consider gravity waves and then capillary–gravity waves with surfactants. In both cases, the analyses are pertinent to wave packets with narrow-banded spectra. In typical ocean wave spectra, one might expect that short viscous waves would appear in a broad band; e.g. the wavelets described by Kawai (1979) are probably more broad-banded than narrow-banded. However, Henderson & Hammack (1987) observed a narrow-banded spectrum of capillary–gravity waves. Therefore, it is appropriate as a first attempt to describe nonlinear viscous waves by wave-packet equations except for resonant cases, for which separate consideration should be given. For gravity waves, we examine the case when the thickness of the free-surface boundary layer is of the same order as the wave amplitude. For capillary–gravity waves, the boundary-layer thickness is considered to be much smaller than the wave amplitude, but a stronger dissipative effect is exhibited due to the surfactant. In both cases, the resulting equation is a dissipative nonlinear Schrödinger equation (dissipative NLS), which contains a linear dissipation term; the other terms remain unaltered from their counterparts for inviscid flow.

We adopt the multiple-scale method to represent the wave modulation and a boundary-layer scaling to incorporate the effects of viscosity and surfactant. For a water depth that is large in comparison with the length of the wave packet, a slow modulation in the vertical direction must be added, as introduced by McGoldrick (1970) and explained further by Mei (1983). The free-surface boundary layer has been considered in several studies of the mean drift in water waves, each using coordinates such that a boundary-layer variable could be measured from the actual location of the free surface. Longuet-Higgins (1953) and Liu & Davis (1977) used a local curvilinear coordinate system moving with the free surface, Phillips (1966) and Craik (1982) chose a conformal transformation, and Ünlüata & Mei (1970) introduced a Lagrangian system. In the present study, our goal is somewhat different, and the analysis is extended to higher order. One choice of coordinates that we considered initially was an orthogonal system obtained from a higher-order conformal transformation. It appeared to us, however, that a more straightforward formulation can be achieved by a non-orthogonal system with one coordinate measured horizontally and the other measured vertically from the exact location of the free surface.

The formulation for two-dimensional capillary–gravity waves is developed in §2, where the coordinate system and governing equations are presented. Suitable variables for the methods of multiple scales and matched asymptotic expansions are introduced, and the first-order inner and outer solutions are derived. In §3, a dissipative NLS equation is derived for viscous gravity waves with slowly varying amplitude; in §4, capillary effects are added. The resulting dissipative NLS equation describes the effect of surfactants on the evolution of weakly nonlinear waves. Non-uniformities associated with the second- and the third-harmonic resonances and with pure capillary waves are discussed. Numerical solutions to the dissipative NLS equations are obtained in §5, showing the modulation of viscous wave envelopes in the presence of surfactants.

2. Formulation

We consider the slow evolution of two-dimensional surface waves influenced by an insoluble surfactant as well as by dispersion and weak nonlinearity. The extent of the wave packet is taken to be small in comparison with the fluid depth, so that the depth may be regarded as infinite. The fluid below the free surface has constant density ρ and viscosity μ, and the air above the free surface will be ignored. The surfactant is characterized by a surface-dilational modulus M, which measures the resistance to the compression/expansion type of surface deformation (Lucassen 1982). Changes in surfactant concentration cause the surface tension σ to vary in time and space. The flow is caused by initial surface disturbances with small but finite amplitude, and is irrotational everywhere except in the boundary layer beneath the free surface, since the viscosity is considered to be small.

In general, the boundary-layer thickness may be much smaller than the wave amplitude. Since the boundary-layer part of the solution is expressed in terms of an inner variable measured from the surface, matching with an outer potential-flow solution is facilitated by the introduction of a coordinate system that moves with the free surface. One such system is a non-orthogonal coordinate system (x, y) generated by subtracting the free-surface elevation η from the vertical coordinate of a Cartesian system (x', y'):

$$x = x', \quad y = y' - \eta(x, t), \tag{2.1}$$

where $\eta(x,t) = \eta(x',t)$, and y is directed upward from the mean free surface. The two components of the momentum equation are obtained by applying (2.1) to the non-dimensional Navier–Stokes equations expressed in the Cartesian coordinate system (x',y'):

$$u_t + uu_x + (v - \eta_t - u\eta_x)\,u_y = -p_x + \eta_x p_y + \epsilon[u_{xx} + (1+\eta_x^2)\,u_{yy} - 2\eta_x u_{xy} - \eta_{xx} u_y], \tag{2.2a}$$

$$v_t + uv_x + (v - \eta_t - u\eta_x)\,v_y = -p_y + \epsilon[v_{xx} + (1+\eta_x^2)\,v_{yy} - 2\eta_x v_{xy} - \eta_{xx} v_y]. \tag{2.2b}$$

Here, the reciprocals of the wavenumber k and the frequency ω_0 of the linear fundamental wave are used as the length and time scales, respectively. The horizontal and vertical velocity components u and v are scaled by ω_0/k, and the pressure p (with the hydrostatic component subtracted) is scaled by $\rho\omega_0^2/k^2$. Since the velocity vector is still written using the base vectors of the Cartesian coordinate system (x',y'), only the chain rule has been used to derive (2.2). The reciprocal of the Reynolds number, which is the primary small parameter, is defined as $\epsilon = k^2\mu/(\rho\omega_0)$. From the continuity equation for constant density, we have

$$u_x - \eta_x u_y + v_y = 0. \tag{2.3}$$

If the elements of the non-dimensional stress tensor referred to the (x',y') coordinate system are denoted by τ_{ij}, and n_1 and n_2 are the x' and y' components of the unit vector normal to the surface, the surface force per unit area has x' and y' components F_1 and F_2 given by $F_i = \tau_{ij} n_j$. Since the slope of the free surface is η_x, the components of the outward normal are $n_1 = -\eta_x/L$ and $n_2 = 1/L$, where $L = (1+\eta_x^2)^{\frac{1}{2}}$. The normal and tangential stresses then become $F_i n_i$ and $F_i t_i$, where $t_1 = n_2$ and $t_2 = -n_1$. The normal stress on the free surface should balance the product of the curvature and the surface-tension coefficient when the pressure above the free surface is taken to be zero. In the present coordinate system, this condition is expressed as

$$p = \frac{2\epsilon}{L^2}[\eta_x^2(u_x - \eta_x u_y) - \eta_x(u_y + v_x) + (1+\eta_x^2)\,v_y] + G\eta - \frac{T}{L^3}\eta_{xx} \quad \text{at} \quad y = 0, \tag{2.4}$$

where $G = kg/\omega_0^2$ and $T = k^3\sigma/(\rho\omega_0^2)$. Here, g is the gravitational acceleration acting vertically downward, and σ is the local surface-tension coefficient. The boundary condition (2.4) is applied at the free surface which is exactly $y = 0$ due to the transformation (2.1).

The tangential stress on the free surface balances the surface-tension gradient σ_s, induced by the surfactant. If we assume that the surface tension σ is a function only of the local surfactant concentration $\bar{\Gamma}$, we have, in dimensional form:

$$\sigma_s = \frac{d\sigma}{d\bar{\Gamma}}\frac{\partial\bar{\Gamma}}{\partial s} = -\frac{M}{\Gamma_0}\frac{\partial\bar{\Gamma}}{\partial s}, \tag{2.5}$$

where s is a coordinate along the surface,

$$M \equiv -\Gamma_0 \left.\frac{d\sigma}{d\bar{\Gamma}}\right|_{\bar{\Gamma}=\Gamma_0}$$

is the surface dilational modulus, and Γ_0 is the surfactant concentration for the undisturbed surface. In the definition of M, a local linear approximation for the surface-tension variation has been used near σ_0, the undisturbed value for the

surface-tension coefficient; thus $\sigma = \sigma_0 - M(\bar{\Gamma} - \Gamma_0)/\Gamma_0$. Since the surface-tension coefficient variations do not occur in the normal-stress boundary condition (2.4) to the order considered here, we may replace T by T_0, the undisturbed surface-tension coefficient. The required surface shear-stress condition then becomes

$$2\eta_x(v_y - u_x + \eta_x u_y) + (1-\eta_x^2)(u_y + v_x - \eta_x v_y) = -\frac{\bar{\kappa}}{\epsilon} L\Gamma_x \quad \text{at} \quad y = 0, \tag{2.5}$$

where $\bar{\kappa} = k^3 M/\rho\omega_0^2$ and $\Gamma = \bar{\Gamma}/\Gamma_0$ are, respectively, the non-dimensional surface dilational modulus and surfactant concentration.

When the surfactant is insoluble and non-diffusive (no diffusion along the surface nor to and from the bulk fluid), the mass in a surface material element is conserved, or $\mathrm{D}(\bar{\Gamma}\Sigma)/\mathrm{D}t = 0$, where $\mathrm{D}/\mathrm{D}t$ indicates a material derivative and Σ is the area of the associated surface material element. The surfactant conservation equation (van den Tempel & van de Riet 1965) in the present coordinate system simplifies to

$$\Gamma_t + u\Gamma_x = -\frac{\Gamma}{L^2}(u_x + \eta_x v_x). \tag{2.7}$$

The governing equations are completed with the kinematic condition:

$$v = \eta_t + u\eta_x \quad \text{at} \quad y = 0. \tag{2.8}$$

We also require the wave amplitude to be small as measured by a, the initial amplitude of the fundamental mode. The relative importance of nonlinearity, surfactant, and viscosity is determined through the scaling of a, κ, and ϵ, respectively. Here, we choose $\tilde{\kappa} = \epsilon^{\frac{1}{2}}$, where $\kappa = O(1)$, to observe the dissipative effect of surfactants in the first approximation. This scaling allows the surfactant concentration to be near the value that causes maximum damping, and thus provides the most interesting limit. If $\tilde{\kappa}$ is scaled to be much larger, our analysis gives a constant damping coefficient that is recovered simply by taking $\kappa \to \infty$ using the present scaling. For a wave with the minimum wave speed ($G = T_0$), water with $\rho = 1000\ \mathrm{kg/m^3}$, $g = 9.8\ \mathrm{m/s^2}$, and $\sigma_0 = 0.074\ \mathrm{N/m}$, has the value $\epsilon^{\frac{1}{2}} \approx 0.04$. A surface pressure (change in surface-tension coefficient from the undisturbed value) of 0.006 N/m is possible in a ship wake and M might be as large as 0.03 n/n, depending on the nature of the surfactant (Lucassen-Reynders & Lucassen 1969). For these values, κ is approximately 5, which we consider to be $O(1)$. The relationship between a and the boundary-layer thickness, which is $O(\epsilon^{\frac{1}{2}})$, is chosen to determine the viscous effects in the amplitude equation at third order.

We introduce the slow variables

$$\tau = a^2 t, \quad \xi = a(x - c_g t), \quad \bar{y} = ay, \tag{2.9}$$

where c_g denotes the group velocity of the primary progressive wave. The first two small scales are identical to those used by Davey & Stewartson (1974) and Djordjevic & Redekopp (1977) for an inviscid fluid with finite depth. The slow modulation in the vertical direction is added to suppress the inconsistency in the third-order solutions for infinite depth, as explained by Mei (1983) for an inviscid fluid. The slow variation in the horizontal direction thus requires a corresponding long-scale variation in the vertical direction, and the non-dimensional depth is taken to be much larger than the extent of the wave packet, which is $O(a^{-1})$.

The flow outside the boundary layer can be described by a velocity potential ϕ, which should satisfy the Laplace equation. In the present coordinate system,

$$\phi_{xx} + \phi_{yy} = 2\eta_x \phi_{xy} + \eta_{xx}\phi_y - \eta_x^2 \phi_{yy}. \tag{2.10}$$

We expand the velocity potential ϕ for small amplitude a:

$$\phi = a\phi_1 + a^2\phi_2 + a^3\phi_3 + \ldots. \tag{2.11}$$

By introducing the slow variables (2.9) and substituting the expansion (2.11) into (2.10), we obtain a sequence of equations for the ϕ_i. The lowest-order equation is the Laplace one, while higher-order equations are Poisson ones with derivatives of the lowest-order terms providing the forcing. The lowest-order equation gives

$$\phi_1 = (AE + A^cE^{-1})\,e^y + \phi_1^0(\xi, \bar{y}, \tau), \tag{2.12}$$

where $E \equiv \exp\{i(x-t)\}$ and the superscript c denotes the complex conjugate. The function $A(\xi, \tau)$ describes a slow variation of amplitude with a mean value of $\frac{1}{2}$ at $\tau = 0$, since a is the initial amplitude of this mode. Since the factor e^y in (2.12) decays exponentially with depth, the slowly varying amplitude A need not depend on $\bar{y}$. The long-scale velocity potential $\phi_1^0(\xi, \bar{y}, \tau)$ satisfies the Laplace equation in ξ and $\bar{y}$ to avoid secular terms arising from the equation for ϕ_3. Also, the boundary condition $\phi_{1\bar{y}}^0 = 0$ at $\bar{y} = 0$ should be imposed to suppress secular terms in the second-order free-surface elevation η_2 below. In the present study, we set $\phi_1^0 = 0$. An example of non-zero ϕ_1^0 for a time-varying current is given by Mei (1983).

The velocity components are obtained from the gradient of the velocity potential (2.11) in the x' and y' coordinates with the transformation (2.1):

$$u = ai(AE - A^cE^{-1})\,e^y + a^2(\phi_{2x} + \phi_{1\xi} - \eta_{1x}\phi_{1y}) + \ldots, \tag{2.13a}$$

$$v = a(AE + A^cE^{-1})\,e^y + a^2\phi_{2y} + a^3(\phi_{3y} + \phi_{2\bar{y}}) + \ldots. \tag{2.13b}$$

From the Bernoulli equation, the pressure for the outer region of irrotational flow is

$$p = ai(AE - A^cE^{-1})\,e^y - a^2[\phi_{2t} - c_g\phi_{1\xi} - \eta_{1t}\phi_{1y} + \tfrac{1}{2}(\phi_{1x}^2 + \phi_{1y}^2)] - a^3[\phi_{3t} - c_g\phi_{2\xi} + \phi_{1\tau} - \eta_{1t}\phi_{2y} + (\phi_{2y} - \eta_{2t} + c_g\eta_{1\xi})\phi_{1y} + (\phi_{2x} + \phi_{1x})\phi_{1x} - \eta_{1x}\phi_{1x}\phi_{1y}] + \ldots. \tag{2.14}$$

In the boundary layer, the system (2.2)–(2.8) is solved after introducing the slow variables (2.9) and the inner coordinate

$$y^* = \frac{y}{\epsilon^{\frac{1}{2}}} \tag{2.15}$$

and expanding the velocity components, pressure surfactant concentration, and free-surface elevation for large Reynolds number. The gauge functions for the inner expansions are to be determined in a stepwise manner after the scale of the amplitude is chosen. The differential equations for the first-order boundary-layer quantities u_1^*, ψ_1^*, p_1^*, and Γ_1 are independent of the amplitude scale, with the boundary condition for u_1^* obtained by differentiating (2.6) with respect to time and applying (2.7). The solutions must also match with the outer solutions found from (2.13)–(2.14). The first-order inner solutions, surfactant concentration Γ_1, and surface elevation η_1 become

$$\eta_1 = p_1^* = iv_1^* = iAE + \text{c.c.}, \tag{2.16a}$$

$$u_1^* = (Q_1 + i)\,AE + \text{c.c.}, \tag{2.16b}$$

$$\Gamma_1 = (Q_0 + i)\,AE + \text{c.c.}, \tag{2.16c}$$

where $$Q_0 = \frac{\sqrt{2\kappa}}{1 - i(1 - \sqrt{2\kappa})}, \quad Q_1 = Q_0 \exp\left(\frac{1-i}{\sqrt{2}}y^*\right),$$

and c.c. denotes the complex conjugate. The linear dispersion equation

$$G+T_0=1 \tag{2.17}$$

is obtained from the boundary and matching conditions for the pressure and is not affected by surfactants.

Further development of the solutions to (2.2)–(2.8) is summarized in the following sections. A more complete development of the algebraic details is given by Joo (1989). At third order, where we terminate the analysis, the matching condition yields the evolution equation for $A(\xi,\tau)$ in the form of a dissipative NLS equation that includes the effects of viscosity, surface tension, and surfactant.

3. Gravity waves

We first examine the case when the capillary effect is absent; i.e. we take $T=\Gamma=0$ and then, by necessity, $\kappa=0$. The wave amplitude is chosen to be of the same order as the boundary-layer thickness, so that

$$\lambda a=\epsilon^{\frac{1}{2}}, \tag{3.1}$$

where λ is an $O(1)$ proportionality constant. For the first few terms, it can be verified that the gauge functions for the inner expansions are

$$\delta_i(\epsilon)=\left(\frac{\epsilon^{\frac{1}{2}}}{\lambda}\right)^i, \tag{3.2}$$

where λ is inserted for convenience. The first-order inner and outer solutions are identical to those in the previous section except that G is replaced by unity, and Q_1 in (2.16*b*) is absent; thus u_1^* is independent of y^*.

The second-order term, $O(\epsilon)$, in the potential is found to be

$$\phi_2=\mathrm{i}A^2E^2\,\mathrm{e}^{y}-\mathrm{i}A_\xi Ey\,\mathrm{e}^{y}+\text{c.c.}+\phi_2^0(\xi,\bar{y},\tau). \tag{3.3}$$

The solution to the homogeneous equation, $F_2(\xi,\bar{y},\tau)E^2\,\mathrm{e}^{2y}+F_1(\xi,\bar{y},\tau)E\,\mathrm{e}^{y}+\text{c.c.}$, is not included. Matching shows that $F_2=0$. The other coefficient F_1 is set equal to zero; taking $F_1\neq 0$ would be equivalent to changing A by an amount aF_1. The long-scale velocity potential ϕ_2^0 satisfies the Laplace equation in ξ and $\bar{y}$ which can be obtained by extending the expansions of the irrotationality condition to the fourth order. (From another viewpoint, the flow at large distances such that $\xi=O(1)$ and $\bar{y}=O(1)$ is described in this way.) The boundary condition for ϕ_2^0 will be determined at third order. The second-order velocity components and the pressure in the outer region are found from (2.13)–(2.14). In the boundary layer, the second-order equations are found from the expansions of (2.2)–(2.8). After matching with the outer solutions, the second-order solutions become

$$v_2^*=\lambda AEy^*+\mathrm{i}A^2E^2-\mathrm{i}A_\xi E+\text{c.c.}, \tag{3.4a}$$

$$\eta_2=-A^2E^2+\tfrac{1}{2}A_\xi E+\text{c.c.}, \tag{3.4b}$$

$$p_2^*=\mathrm{i}\lambda AEy^*-A^2E^2+\tfrac{1}{2}A_\xi E+\text{c.c.}, \tag{3.4c}$$

$$u_2^*=\lambda\sqrt{2}(1-\mathrm{i})\exp\left(\frac{1-\mathrm{i}}{\sqrt{2}}y^*\right)AE+\mathrm{i}\lambda AEy^*-A^2E^2+A_\xi E+\text{c.c.}+2|A|^2. \tag{3.4d}$$

A long-scale free-surface elevation $\eta_2^0(\xi,\tau)$ that could appear in ((3.4*b*) as an integration constant has been set equal to zero as a consequence of matching the

pressures. The group velocity c_g has been replaced by $\frac{1}{2}$, again so that the pressures can be matched.

The differential equation for ϕ_3 is found from the third-order terms in (2.10). The solution to the homogeneous equation is dropped for the same reason as cited for ϕ_2. The solution then has the form

$$\phi_3 = -\tfrac{3}{2}A^3E^3\,\mathrm{e}^y + AA_\xi E^2(\tfrac{3}{2}\mathrm{e}^y + y\,\mathrm{e}^y) - AA_\xi^c(\tfrac{1}{2}\mathrm{e}^y + y\,\mathrm{e}^y) - \tfrac{1}{2}A_{\xi\xi}Ey^2\,\mathrm{e}^y + \text{c.c.} + \phi_3^0(\xi,\bar{y},\tau). \tag{3.5}$$

The outer solutions v_3 and p_3 for the $O(\epsilon^{\frac{3}{2}})$ terms in the vertical component of the velocity and the hydrodynamic pressure are then obtained from (2.13b) and (2.14)

The solution v_3^* for the boundary layer at third order is, after matching with (2.13b),

$$v_3^* = -\lambda\sqrt{2}(1-\mathrm{i})\exp\left(\frac{1-\mathrm{i}}{\sqrt{2}}y^*\right)\left(A^2E^2 - \frac{1-\mathrm{i}}{\sqrt{2}}\lambda AE + |A|^2\right) + \lambda\,\mathrm{i}A^2E^2y^*$$

$$+\lambda^2\tfrac{1}{2}AEy^{*2} - 2\mathrm{i}\lambda AA_\xi Ey^* - \tfrac{3}{2}A^3E^3 + \tfrac{5}{2}AA_\xi E^2 - \tfrac{3}{2}AA_\xi^c + \text{c.c.} + \phi_{2\bar{y}}^0. \tag{3.6}$$

The third-order free-surface elevation then becomes

$$\eta_3 = -\tfrac{3}{2}\mathrm{i}A^3E^3 + 3\mathrm{i}|A|^2AE + 2\lambda^2AE + 2\mathrm{i}AA_\xi E^2 + \tfrac{1}{4}\mathrm{i}A_{\xi\xi}E + A_\tau E + \eta_3^0(\xi,\tau), \tag{3.7}$$

where the condition

$$\phi_{2\bar{y}}^0 = 2\frac{\partial|A|^2}{\partial\xi} \quad \text{at} \quad \bar{y} = 0 \tag{3.8}$$

has been imposed to suppress secular terms. The equations for p_3^* obtained from (2.2b) can be solved with the boundary condition generated from (2.4) to yield

$$p_3^* = \tfrac{1}{2}\mathrm{i}\lambda^2AEy^{*2} - \lambda A^2E^2y^* + \tfrac{3}{2}\lambda AA_\xi Ey^* + 4\lambda^2AE - \tfrac{3}{2}\mathrm{i}A^3E^3 + 3\mathrm{i}|A|^2AE$$

$$+2\mathrm{i}AA_\xi E^2 + \tfrac{1}{4}\mathrm{i}A_{\xi\xi}E + A_\tau E + \text{c.c.} - 2\lambda|A|^2y^* + \eta_3^0(\xi,\tau). \tag{3.9}$$

The matching condition for this pressure with the outer solution (2.14) finally gives

$$\eta_3^0(\xi,\tau) = \tfrac{1}{2}\phi_{2\xi}^0 \quad \text{at} \quad \bar{y} = 0 \tag{3.10}$$

for terms independent of E, and

$$A_\tau + 2\lambda^2A + \tfrac{1}{8}\mathrm{i}A_{\xi\xi} = -2\mathrm{i}\,|A|^2A \tag{3.11}$$

for terms linear in E.

Except for the additional term $2\lambda^2A$, the amplitude equation (3.11) is identical to the NLS equation that governs the amplitude modulation of gravity waves in inviscid flow. It is thus appropriate to call the amplitude equation a dissipative NLS equation. From (3.11), the integral of $|A|^2$ with respect to ξ is easily found to decay as $\exp(-4\lambda^2\tau)$.

For infinite wavetrains independent of ξ, the solution $A_0(\tau)$ of (3.11) that satisfies $A_0(0) = a_0$ is

$$A_0(\tau) = a_0\exp\left[-2\lambda^2\tau + \frac{\mathrm{i}}{2\lambda^2}|a_0|^2(\mathrm{e}^{-4\lambda^2\tau} - 1)\right], \tag{3.12}$$

where a_0 is a complex constant with $|a_0| = \frac{1}{2}$, as explained earlier. Here, the expression $|a_0|^2$ is kept to show the amplitude dependence explicitly. In the inviscid limit, $\lambda \to 0$, the Stokes wave (to third order) is recovered. The decaying factor in (3.12), combined with (2.9) and (3.1), becomes $\exp(-2\epsilon t)$. Thus, the damping coefficient D_g

for weakly nonlinear gravity waves is $D_g = 2\epsilon$, which is identical to the linear result of Stokes (1845). In retrospect, we could instead have shown that the damping coefficient is unaffected by nonlinearity at this order using the dissipation function and its expansion for small amplitude. Viscosity also causes a phase shift, as can be seen from (3.12).

4. Capillary–gravity waves

We now consider capillary–gravity waves with a surfactant on the free surface. For the gravity wave in the previous section, the amplitude of the wave is chosen to be of the same order as the boundary-layer thickness so that nonlinearity and dissipation both appear in the amplitude equation. When a surfactant is present, however, lower-order dissipation is expected; thus, the amplitude is chosen to be of lower order than the boundary-layer thickness:

$$\lambda a = \epsilon^{\frac{1}{4}}, \tag{4.1}$$

where λ is again a proportionality constant. The gauge functions for the inner expansions now become

$$\delta_i(\epsilon) = \left(\frac{\epsilon^{\frac{1}{4}}}{\lambda}\right)^i. \tag{4.2}$$

The first-order solutions, $O(\epsilon^{\frac{1}{4}})$, are given by (2.13)–(2.14) for the outer region of irrotational flow and by (2.16) for the boundary layer. Since the non-dimensional surface dilational modulus κ and the Weber number T_0 are non-zero, the boundary-layer solutions for the horizontal velocity component and displacement are affected by the surfactant at the leading order, and the linear dispersion relationship (2.17) is that for capillary–gravity waves.

The equation for the $O(\epsilon^{\frac{1}{2}})$ term ϕ_2 in the velocity potential is identical to that for the gravity wave (because ϕ_1 and η_1 are identical), but the appropriate solution now includes a solution of the homogeneous equation:

$$\phi_2 = FE^2 e^{2y} + iA^2E^2 e^{y} - iA_\xi E y e^{y} + \text{c.c.} + \phi_2^0(\xi, \bar{y}, \tau), \tag{4.3}$$

where $F(\xi, \tau)$ can be determined through matching. Again, the long-scale potential ϕ_2^0 should satisfy the Laplace equation, with the boundary condition to be determined through matching of the third-order solutions.

The boundary-layer equations and boundary conditions for the $O(\epsilon^{\frac{1}{2}})$ terms are found as before by substituting the expansions into (2.2) – (2.8). Some of the terms are different from those for gravity waves because the boundary-layer thickness is now small in comparison with the wave amplitude. Only the main results are shown here; details are given by Joo (1989).

After determining the vertical velocity component v_2^* as before, the second-order free-surface elevation becomes

$$\eta_2 = iFE^2 - A^2E^2 + (1 - c_g) A_\xi E + \text{c.c.}, \tag{4.4}$$

where the long-scale quantity $\eta_2^0(\xi, \bar{y}, \tau)$ is omitted in anticipation of the matching condition for the second-order pressure. After (4.4) is substituted into the boundary condition for p_2^*, the inner solution for the second-order pressure is obtained:

$$p_2^* = (1 + 3T_0)(iF - A^2)E^2 + (1 - c_g + 2T_0) A_\xi E + \text{c.c.} \tag{4.5}$$

Matching (4.5) with the outer solution (2.14) gives the slowly varying amplitude F and the group velocity c_g as

$$F = \frac{\mathrm{i}3T_0}{1-3T_0}A^2, \tag{4.6}$$

$$c_g = \tfrac{1}{2}(1+2T_0), \tag{4.7}$$

respectively. It is noteworthy that η_2 and p_2^* are not affected by viscosity and surfactant. Since the amplitude a is taken to be much larger than the boundary-layer thickness $\epsilon^{\frac{1}{2}}$, nonlinearity is dominant; the correction due to viscosity or surfactant on surface elevation and surface pressure first appear at third order. The group velocity (4.7) thus agrees with the relationship for a linear capillary–gravity wave in inviscid flow. Also, F blows up as $T_0 \to \frac{1}{3}$; a second-harmonic resonance persists in the presence of dissipative effects. A complete discussion of this resonant behaviour was given by McGoldrick (1970). A modified asymptotic flow description for small values of $|T_0 - \frac{1}{3}|$ is discussed below.

The boundary-layer solution for u_2^* is affected by the nonlinear behaviour of the surfactant. However, η_3 and p_3^* are not affected by u_2^* for the same reason as mentioned above. The solution for u_2^* thus is omitted.

Terms $O(\epsilon^{\frac{3}{2}})$ in (2.10) give the differential equation for the third-order potential ϕ_3. The appropriate solution is

$$\begin{aligned}\phi_3 = {} & F_3 E^3 \mathrm{e}^{3y} + F_2 E^2 \mathrm{e}^{2y} - A^3 E^3 \left[\frac{3(1-T_0)}{2(1-3T_0)}\mathrm{e}^{y} + \frac{6T_0}{1-3T_0}\mathrm{e}^{2y}\right] + |A|^2 AE \frac{6T_0}{1-3T_0}\mathrm{e}^{2y} \\ & + AA_\xi E^2\left(\frac{3-2T_0}{2}\mathrm{e}^{y} + y\,\mathrm{e}^{y} + \frac{6T_0}{1-3T_0}y\,\mathrm{e}^{2y}\right) - AA_\xi^c\left(\frac{1-2T_0}{2}\mathrm{e}^{y} + y\,\mathrm{e}^{y}\right) \\ & - \tfrac{1}{2}A_{\xi\xi}Ey^2\,\mathrm{e}^{y} + \text{c.c.} + \phi_3^0(\xi, \bar{y}, \tau),\end{aligned} \tag{4.8}$$

where the slowly varying amplitudes $F_3(\xi,\tau)$ and $F_2(\xi,\tau)$ are to be determined from the matching condition. As in the derivation of ϕ_2, a first-harmonic term in the solution to the homogeneous equation is dropped. The vertical velocity component v_3 is then obtained from (2.13b), and (2.14) yields the third-order pressure:

$$\begin{aligned}p_3 = {} & \mathrm{i}3F_3E^3\mathrm{e}^{3y} + \mathrm{i}2F_2E^2\mathrm{e}^{2y} - \mathrm{i}A^3E^3\left[\frac{5-9T_0}{2(1-3T_0)}\mathrm{e}^{y} - \frac{1-21T_0}{1-3T_0}\mathrm{e}^{2y} - \frac{6T_0}{1-3T_0}\mathrm{e}^{3y}\right] \\ & + \mathrm{i}AA_\xi E^2\left[3\,\mathrm{e}^{y} + 2y\,\mathrm{e}^{y} - \frac{1-6T_0-6T_0^2}{1-3T_0}\mathrm{e}^{2y} - \frac{1-15T_0}{1-3T_0}y\,\mathrm{e}^{2y}\right] \\ & + \mathrm{i}|A|^2AE\left[\frac{2}{1-3T_0}\mathrm{e}^{y} - \frac{3(1-5T_0)}{1-3T_0}\mathrm{e}^{2y} - \frac{6T_0}{1-3T_0}\mathrm{e}^{3y}\right] - \mathrm{i}A_{\xi\xi}E\left(\frac{y^2}{2}\mathrm{e}^{y} + \frac{1+2T_0}{2}y\,\mathrm{e}^{y}\right) \\ & + \mathrm{i}AA_\xi^c(\mathrm{e}^{y} - \mathrm{e}^{2y} - y\,\mathrm{e}^{2y}) - A_\tau E\,\mathrm{e}^{y} + \text{c.c.} + (\eta_{1t} - \phi_{1y})\phi_{2y} + c_g\phi_{2\xi}^0.\end{aligned} \tag{4.9}$$

The third-order boundary-layer solutions are again obtained from the continuity equation (2.3) for v_3^*, the free-surface boundary condition (2.8), and the vertical momentum equation (2.2b) for p_3^*. The third-order free-surface elevation η_3 is then obtained as

$$\begin{aligned}\eta_3 = {} & \mathrm{i}\left[F_3 - \frac{3(1+3T_0)}{2(1-3T_0)}A^3\right]E^3 + \left[\mathrm{i}F_2 + \left\{\mathrm{i}\frac{6T_0^2-13T_0+4}{2(1-3T_0)} + \tfrac{1}{2}Q_0\right\}AA_\xi\right]E^2 \\ & + \frac{3(1+T_0)}{1-3T_0}\mathrm{i}|A|^2AE + (\tfrac{1}{4}-T_0^2)\,\mathrm{i}A_{\xi\xi}E + A_\tau E + \frac{1+\mathrm{i}}{\sqrt{2}}Q_0AE + \text{c.c.} + \eta_3^0,\end{aligned} \tag{4.10}$$

where the condition

$$\phi^0_{2\bar{y}} = 2(1-T_0)\,|A^2|_\xi - \mathrm{i}(Q_0 A A^{\mathrm{c}}_\xi - Q^{\mathrm{c}}_0 A^{\mathrm{c}} A_\xi) \quad \text{at} \quad \bar{y}=0 \tag{4.11}$$

has been imposed to suppress secular terms. As mentioned earlier, (4.11) is the boundary condition for ϕ^0_2; thus, ϕ^0_2 is uniquely determined once A is obtained from (4.15) below. Additional nonlinear forcing terms are present in (4.11) because of the surfactant.

Solving the differential equation for p^*_3 with the associated boundary condition results in

$$\begin{aligned} p^*_3 = {} & \mathrm{i}\left[(1+8T_0)F_3 - \frac{3(1+12T_0+21T_0^2)}{2(1-3T_0)}A^3\right]E^3 + \mathrm{i}(1+3T_0)F_2E^2 \\ & + \left[\mathrm{i}\frac{(1+3T_0)(4-13T_0+6T_0^2)+16T_0}{2(1-3T_0)} + \frac{1+3T_0}{2}Q_0\right]AA_\xi E^2 + \lambda^2\left(\mathrm{i}y^* + \frac{1+\mathrm{i}}{\sqrt{2}}Q_0\right)AE \\ & + \mathrm{i}\frac{1-8T_0+4T_0^2}{4}A_{\xi\xi}E + A_\tau E + \mathrm{i}\frac{6+3T_0+9T_0^2}{2(1-3T_0)}|A|^2AE + \mathrm{c.c.} + G\eta^0_3. \end{aligned} \tag{4.12}$$

Applying the matching condition for the pressure, we determine F_2 and F_3:

$$F_2 = \left[\frac{3T_0(7-15T_0+6T_0^2)}{2(1-3T_0)^2} - \mathrm{i}\frac{1+3T_0}{2(1-3T_0)}Q_0\right]AA_\xi, \tag{4.13a}$$

$$F_3 = -\frac{3T_0(5+21T_0)}{4(1-3T_0)(1-4T_0)}A^3. \tag{4.13b}$$

We also obtain

$$\eta^0_3 = \frac{1+2T_0}{2(1-T_0)}\phi^0_{2\xi}, \tag{4.14}$$

and the amplitude equation for the capillary–gravity wave with viscosity and surfactant:

$$A_\tau + \frac{\lambda^2}{2\sqrt{2}}\frac{\kappa[\kappa+\mathrm{i}(\sqrt{2}-\kappa)]}{\kappa^2-\sqrt{2}\kappa+1}A + \tfrac{1}{8}\mathrm{i}(4T_0^2-8T_0+1)A_{\xi\xi} = -\mathrm{i}\frac{9T_0^2-15T_0+8}{4(1-3T_0)}|A|^2A. \tag{4.15}$$

This is the one-dimensional form of the equation given by Miles (1988), now with the dependence on κ shown explicitly in the coefficient of A.

Two more non-uniformities are observed, in addition to the one for the second-harmonic resonance ($T_0 = \frac{1}{3}$). In (4.13*b*), the amplitude F_3 becomes unbounded as T_0 approaches $\frac{1}{4}$; thus a third-harmonic resonance occurs. As T_0 approaches unity (the value for pure capillary waves), η^0_3 in (4.14) is singular, and a rescaling of the long-scale free-surface elevation is required, as explained below.

The dissipation term proportional to A in (4.15) is associated with the surfactant in the case $\kappa = O(1)$, whereas for a clean surface the dissipation is of higher order, as shown in the previous section where different scaling was required. Therefore, if either λ or κ is zero, the dissipation term in (4.15) is absent, and we recover the amplitude equation for capillary–gravity waves in inviscid flow. The linear term of (4.15) has a complex coefficient; the imaginary part is related to the decay rate, and the real part corresponds to a frequency change due to the surfactant.

A solution of (4.15) for infinite wavetrains which depends only on τ is

$$A_0 = a_0 \exp\left[-\frac{\lambda^2}{2\sqrt{2}}\frac{\kappa^2+\mathrm{i}(\sqrt{2}\kappa-\kappa^2)}{\kappa^2-\sqrt{2}\kappa+1}\tau\right]\exp\left[\mathrm{i}|a_0|^2\left(\frac{9T_0^2-15T_0+8}{1-3T_0}\right)\right.$$
$$\left.\times\left(\frac{\kappa^2-\sqrt{2}\kappa+1}{2\sqrt{2}\kappa^2\lambda^2}\right)\left\{\exp\left(-\frac{1}{\sqrt{2}}\frac{\kappa^2\lambda^2}{\kappa^2-\sqrt{2}\kappa+1}\tau\right)-1\right\}\right]. \quad (4.16)$$

Since the slow time is now defined as $\tau = \epsilon^{\frac{1}{2}}t/\lambda^2$ due to (4.1), the damping coefficient D_s for an infinite wavetrain (4.16) becomes

$$D_s = \frac{\sqrt{2}\kappa^2}{4(\kappa^2-\sqrt{2}\kappa+1)}\epsilon^{\frac{1}{2}}, \quad (4.17)$$

which has a maximum at $\kappa = \sqrt{2}$. At this maximum, the frequency shift due to the surfactant disappears. The damping coefficient (4.17) agrees with the result of Levich (1941, 1962) and Lucassen-Reynders & Lucassen (1969) for linear capillary waves, as can be seen by expanding their solutions for large Reynolds number. It is clear from the result that the damping effect is greatly enhanced by the surfactant.

The above results including the evolution equation (4.15) and the damping coefficient (4.17) are obtained for $\bar{\kappa} = O(\epsilon^{\frac{1}{2}})$. However, they are valid even when the non-dimensional surface dilational modulus is not small. In the limit $\kappa \to \infty$, Q_0 becomes $-\mathrm{i}$, u_1^* and Γ_1 vanish on the surface, and the dissipation coefficient D_s becomes $\epsilon^{\frac{1}{2}}/2^{\frac{3}{2}}$. The surface tension in the normal-stress boundary condition again stays constant through the third-order approximation.

In the derivation of these expansions, we have noted that singular behaviour appears for certain values of the Weber number. The case for $T_0 = \frac{1}{3}$ corresponds to second-harmonic resonance and is related to Wilton's ripples. The non-uniformity can be removed by considering a superposition of the fundamental wave and its second harmonic in the first approximation and by adding an intermediate slow timescale, as in McGoldrick (1970) for inviscid flow. We start by considering a Weber number near the resonance value:

$$T_0 = \tfrac{1}{3} + a\tilde{T}, \quad (4.18)$$

where $\tilde{T} = O(1)$ is a constant. An appropriate solution for ϕ_1 is now

$$\phi_1 = A_1(\xi, \tilde{t})\, E\, \mathrm{e}^{y} + A_2(\xi, \tilde{t})\, E^2\, \mathrm{e}^{2y} + \text{c.c.}, \quad (4.19)$$

instead of (2.12), where

$$\tilde{t} = at = \tau/a \quad (4.20)$$

is the new time variable. The subsequent analysis proceeds as before except for the added complexity due to the presence of second-harmonic terms in the first-order solutions. For example, an appropriate solution of the homogeneous equation for ϕ_2 should include third- and fourth-harmonic terms. A matching condition for the second-order pressure finally gives

$$A_{1\tilde{t}} = -A_1^{\mathrm{c}} A_2 \quad (4.21a)$$
$$A_{2\tilde{t}} + \mathrm{i}\tfrac{3}{2}\tilde{T} + \tfrac{1}{3}A_{2\xi} = \tfrac{1}{2}A_1^2, \quad (4.21b)$$

in addition to the group velocity $c_g = \frac{5}{6}$, the correct value when $T_0 = \frac{1}{3}$.

The evolution equations (4.21) are equivalent to the second-harmonic resonance equations given by McGoldrick (1970), except that a term proportional to $\tilde{T}$ is added to account for values of the Weber number close to $\frac{1}{3}$. The coefficients for the terms with spatial variation are different because the slow variable ξ is constant at points moving with the group velocity; adding $c_g\,\partial/\partial\xi$ to $\partial/\partial\tilde{t}$ leads to the same terms as in

McGoldrick (1970). For large $|\tilde{T}|$, equations (4.21) are consistent with previous results. As $|\tilde{T}| \to \infty$, (4.21*b*) reduces to

$$A_2 = \frac{A_1^2}{3\mathrm{i}\tilde{T}}, \tag{4.22}$$

which, with (4.18), is found to agree with (4.6). Using (4.22) to remove A_2 in (4.21*a*) gives

$$\mathrm{i}A_{1\tilde{t}} = -\frac{1}{3\tilde{T}}|A_1|^2 A_1. \tag{4.23}$$

This equation can also be obtained from (4.15) by using (4.18), setting $\tau = a\tilde{t}$, and noting that the dissipation and the dispersion terms become small as $T_0 \to \frac{1}{3}$. Thus, the results for $T_0 \neq \frac{1}{3}$ and for T_0 close to $\frac{1}{3}$ match asymptotically as $T_0 \to \frac{1}{3}$ and $|T_0 - \frac{1}{3}|/a \to \infty$.

A set of solutions of (4.21) for infinite wavetrains without ξ-dependence can be obtained as

$$A_1 = b_0 \mathrm{e}^{-\mathrm{i}\theta\tilde{t}} \tag{4.24a}$$

$$A_2 = \mathrm{i}\left(\frac{b_0}{b_0^{\mathrm{c}}}\right)\theta \mathrm{e}^{-2\mathrm{i}\theta\tilde{t}}, \tag{4.24b}$$

where

$$\theta = \tfrac{1}{8}[3\tilde{T} - (\operatorname{sgn}\tilde{T})(9\tilde{T}^2 + 16|b_0|^2)^{\frac{1}{2}}], \tag{4.25}$$

and b_0 is a complex constant. The sign in (4.25) has been chosen so that $\theta \to 0$ when $|\tilde{T}| \to \infty$. Then, also $|A_2| \to 0$, and hence b_0 becomes identical to a_0 as $|\tilde{T}| \to \infty$. When $\tilde{T}$ is zero, the wavetrains obtained by McGoldrick (1970) are recovered from (4.24)–(4.25).

A non-uniformity related to the third-harmonic resonance is observed when $T_0 = \frac{1}{4}$. We can expect more non-uniformities for $T_0 = 1/(n+1)$ $(n = 3, 4, \ldots)$, corresponding to nth-harmonic resonance. Uniform expansions near these resonance values of the Weber number can be obtained by modifying those introduced for $T_0 = \frac{1}{3}$ above, as discussed by Dias & Bridges (1990) most recently.

Still another non-uniformity occurs for values of T_0 close to unity, when the surface-tension force is large in comparison with the gravitational force. In this case, the long-wave solutions for the velocity potential and the surface elevation must be modified. Since the orders of magnitude change, it is now convenient to omit subscripts and to denote the largest 'long-wave' terms by $\epsilon^{\frac{1}{2}}\phi^0$ and $\epsilon^{\frac{1}{2}}\eta^0$, where ϕ^0 and η^0 are not necessarily $O(1)$. By repeating the previous derivations when $1 - T_0 \ll 1$, we find that the equations analogous to (4.11) and (4.14) become

$$-\tfrac{1}{2}(1+2T_0)\eta^0_\xi + \phi^0_y = 2(1-T_0)\frac{\partial|A|^2}{\partial\xi} - \mathrm{i}(Q_0 A A^{\mathrm{c}}_\xi - Q_0^{\mathrm{c}} A^{\mathrm{c}} A_\xi) \tag{4.26}$$

$$(1-T_0)\eta^0 = \tfrac{1}{2}(1+2T_0)\epsilon^{\frac{1}{4}}\phi^0_\xi. \tag{4.27}$$

When $1 - T_0 = O(1)$, then $\phi^0 = O(1)$ but $\eta^0 = O(\epsilon^{\frac{1}{4}})$; η^0 and ϕ^0 can be replaced by $\epsilon^{\frac{1}{4}}\eta^0_3$ and ϕ^0_2, respectively, and (4.11) and (4.14) are recovered. When $\epsilon^{\frac{1}{4}} \ll 1 - T_0 \ll 1$, $\eta^0 = O\{\epsilon^{\frac{1}{4}}/(1-T_0)\}$ while ϕ^0 remains $O(1)$. In the distinguished limit corresponding to $1 - T_0 = O(\epsilon^{\frac{1}{4}})$, all terms in (4.26) and (4.27) are retained. Finally, for $1 - \mathrm{T}_0 \ll \epsilon^{\frac{1}{4}}$, $\eta^0 = O(1)$ while $\phi^0 = O(\{(1-T_0)/\epsilon^{\frac{1}{4}}\})$. Thus, for pure capillary disturbances in the presence of a surfactant, there is a long-wave component with a surface elevation $\epsilon^{\frac{1}{2}}\eta^0(\xi, \tau)$, whereas the corresponding long-wave potential is of higher order; η^0 is determined by (4.26). For a clean surface, however, the non-uniformity at $T_0 = 1$ disappears because $Q = 0$ and ϕ^0_2 is proportional to $1 - T_0$.

5. Numerical solution of the dissipative NLS equations

The dissipative NLS equations derived above can describe the evolution of viscous wave envelopes when the Weber number is not too close to the value for three-wave resonances, $T_0 = \frac{1}{3}$. They are special cases of the Ginzburg–Landau equation, which is a generic amplitude equation describing the nonlinear development of unstable waves in many physical systems. Ginzburg–Landau equations have been studied intensively by many authors including Newell & Whitehead (1969), Stewartson & Stuart (1971), Kopell & Howard (1981), and Keefe (1985), often in the context of a dynamical systems approach with just a few spatial modes. The linear stability of periodic-wave solutions was analysed by Stuart & DiPrima (1978) in the absence of dissipation, and generalized by Holmes (1985) and Doering *et al.* (1988) to dissipative systems with complex dispersive and nonlinear coefficients.

In particular, Miles (1988) studied the stability of periodic wavetrains for waves with surfactant, showing that unstable inviscid waves become transiently stable under the influence of dissipation. Joo (1989) performed a similar linear stability analysis using modified Bessel functions and arrived independently at the same stability criteria (when scaled appropriately). These analyses extend the linear stability analysis of Stuart & DiPrima (1978) to incorporate capillary and viscous effects and extend the stability results for inviscid capillary–gravity waves obtained by Djordjevic & Redekopp (1977) to water of infinite depth.

We first consider a perturbation to the wavetrain (3.12) for gravity waves and write

$$A = A_0(\tau)[1 + B_1(\tau)\,e^{il\xi} + B_2(\tau)\,e^{-il\xi}]. \tag{5.1}$$

A norm for one spatial period,

$$N(\tau) = \| |A| - |A_0| \| \equiv \left(\frac{l}{2\pi} \int_{-\pi/l}^{\pi/l} (|A| - |A_0|)^2 \, d\xi \right)^{\frac{1}{2}}, \tag{5.2}$$

can be used as a measure of the growth or decay of the disturbance.

For inviscid flow, the sideband resonance disappears regardless of the disturbance wavenumber when

$$1 - \frac{\sqrt{3}}{2} \leqslant T_0 < \tfrac{1}{3}. \tag{5.3}$$

The corresponding stability analysis for waves in water of finite depth has been reported by Djordjevic & Redekopp (1977). The stability band (5.3) corresponds to the deep-water limit of their stable region, which lies between the minimum phase speed and the second-harmonic resonance. The other stable regions seem to disappear as the depth approaches infinity. Although only neutral stability is predicted for (5.3), large-time computations for this range of T_0 show strikingly different behaviour from that in the other neutrally stable regions, as shown below. When $0 < T_0 < 1 - \sqrt{\frac{3}{2}}$, the lower instability boundary for the disturbance wavenumber l stays at zero, whereas the upper bound increases with T_0 until it blows up at $T_0 = 1 - \sqrt{\frac{3}{2}}$. When the Weber number exceeds the value for the second-harmonic resonance, the upper bound decreases with the Weber number. As $T_0 \to 1$, the upper bound approaches $l = 1/\sqrt{3}$, which is smaller than the value $l = 2\sqrt{2}$ for gravity waves.

Numerical solutions of the NLS equation have been obtained by Yuen & Ferguson (1978) and Weideman & Herbst (1987) and many others, with an emphasis on modulational instability and recurrence of the Fermi–Pasta–Ulam type (Fermi,

Pasta & Ulam 1965). Yuen & Ferguson (1978) examined the relationship between Benjamin–Feir instability and recurrence and showed two types of recurrence, 'simple' and 'complex'. They explained that for modulations with the sideband perturbation wavenumber l in the range $8|a_0|^2 \leqslant l^2 < 32|a_0|^2$ the recurrence is simple because all higher harmonics of the prescribed modulation are stable. For modulations with $0 < l^2 < 8|a_0|^2$, the recurrence is complex (quasi-periodic) because at least one higher harmonic of the prescribed mode lies in the unstable region. Weideman & Herbst (1987) obtained similar solutions using finite-difference, spectral, and pseudospectral methods, and compared the effectiveness of these methods. We use a pseudospectral method to solve the dissipative NLS equations for capillary–gravity waves. This method is appropriate for our purpose, once an aliasing error is suppressed by introducing a sufficient number of degrees of freedom (number of collocation points).

The initial condition (5.1) is specialized to a simple case

$$A = a_0(1 + b\cos l\xi). \tag{5.4}$$

Modulational behaviour for different initial sideband amplitudes, B_1 and B_2, will be discussed later in this section.

A periodic boundary condition

$$A(\xi, \tau) = A\left(\xi + \frac{2\pi}{l}, \tau\right), \tag{5.5}$$

is imposed using a Fourier-collocation method with the computational domain $-\pi/l \leqslant \xi \leqslant \pi/l$. Hence we apply periodic boundary conditions with the same wavelength as the disturbance. The slowly varying amplitude is then expressed as

$$A = \sum_{n=-N}^{N} \tilde{A}_n(\tau)\, \mathrm{e}^{\mathrm{i}n\xi\pi/l}, \tag{5.6}$$

where we choose N as a positive integer power of 2 and a fast Fourier transformation is used to compute the Fourier coefficients $\tilde{A}_n$. As in the analyses, the amplitude of a_0 is $\frac{1}{2}$, and b is small. In particular, we set $a_0 = \tilde{A}_0(0) = 0.5$ and $b = 2\tilde{A}_1(0) = 2\tilde{A}_{-1}(0) = 2\tilde{A}_{-1}(0) = 0.1$ for most of the computations, unless otherwise specified. A fourth-order Hamming modified predictor-corrector method is used for time marching. The fourth-order Runge–Kutta method is used for automatic adjustment of the initial time increment and for computation of starting values. For most computations, the maximum time step is 0.01, and the number of collocation points is 32 for one initial period in ξ.

Figure 1 illustrates the evolution of the Stokes wave for zero viscosity when subject to the modulation described by (5.4). Evolution of the envelope amplitude $|A(\xi, \tau)|$ is shown in figure 1 (a, c and e), whereas the magnitude of each Fourier coefficient $|\tilde{A}_n(\tau)|$ ($n = 0, 1, 2, \ldots$) is plotted in figure 1 (b, d and f). Since $|\tilde{A}_n|$ is symmetric about $n = 0$ owing to (5.4), the evolution for negative n is deleted for clarity. The perturbation wavenumber $l = 1$ corresponds to complex recurrence (figure 1 a, b); $l = 2$ corresponds to the maximum initial growth rate and simple recurrence (figure 1 c, d). These figures agree with the results of Yuen & Ferguson (1978) and Weideman & Herbst (1987), who provide detailed explanations. For the simple recurrence, the fundamental ($n = 0$) and sideband ($n = \pm 1$) modes are periodic, as can be also seen in figure 8. The higher modes (not shown in figure 8), excited due to nonlinear interaction, are not exactly periodic, but they are not

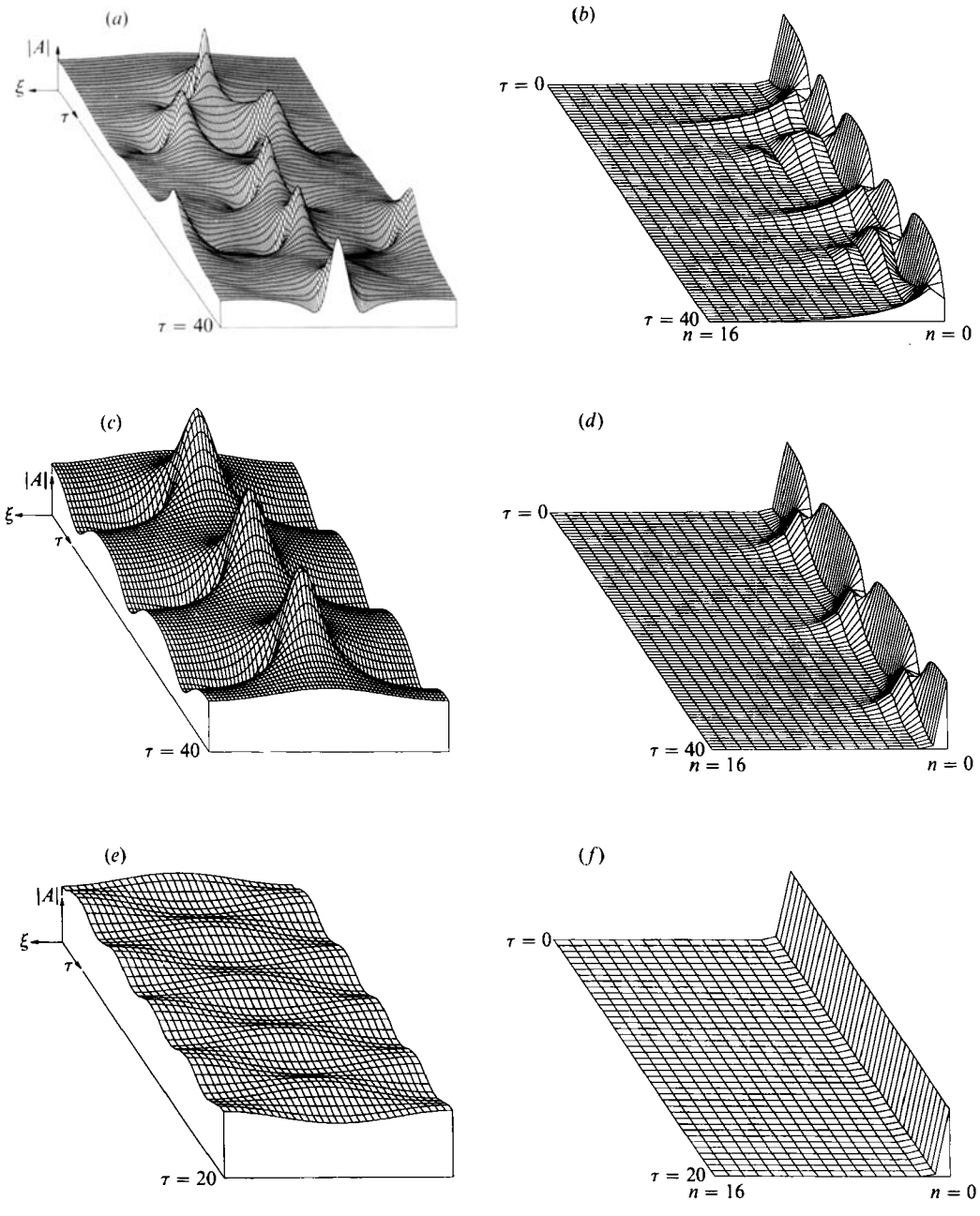

FIGURE 1. Evolution of modulations for inviscid gravity waves ($\lambda = 0$) and perturbation amplitude $b = 0.1$: (*a*) $l = 1$, physical space $-2\pi/l < \xi < 0$; (*b*) $l = 1$, Fourier space; (*c*) $l = 2$, physical space $-2\pi/l < \xi < 0$; (*d*) $l = 2$, Fourier space; (*e*) $l = 4$, physical space $-2\pi/l < \xi < 0$; (*f*) $l = 4$, Fourier space.

dominant at any stage, making the modulation almost periodic in time. When l lies outside of the instability range $0 < l^2 < 32|a_0|^2$, a very nearly periodic oscillation is observed (figure 1*e*), which is in good agreement with the neutral stability predicted by the linear analysis. The corresponding Fourier-space solution (figure 1*f*) shows

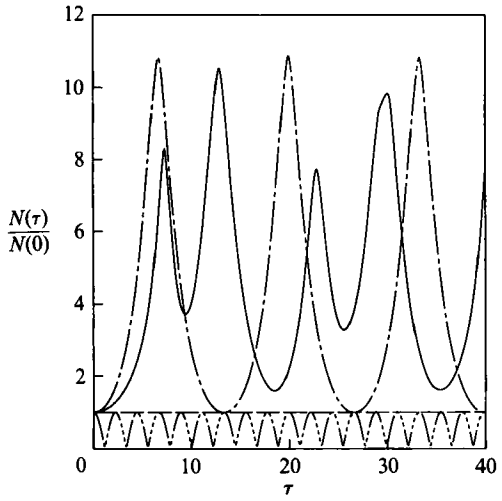

FIGURE 2. Evolution of modulations for gravity waves expressed by $N(\tau)/N(0)$ for $l = 1$ (——), $l = 2$ (— — —), $l = 2\sqrt{2}$ (— — —), and $l = 4$ (·····).

that none of the higher harmonics is excited and that the sidebands never become dominant.

In figure 2, the same cases as in figure 1 are described using the norm N defined in (5.2). The behaviour for small τ is in precise agreement with the linear analysis. The growth rate is a maximum when $l = 2$ and decreases as l increases, resulting in larger recurrence periods, until it becomes zero for $l = 2\sqrt{2}$. When l becomes larger than $2\sqrt{2}$, an oscillation due to neutral stability is observed, as predicted by the linear analysis. When l decreases from 2, the initial growth rate again decreases, but complex recurrence is observed for $l < \sqrt{2}$.

Figure 3 shows the evolution of the slowly varying envelope A gravity waves with small viscosity. The initial condition and the perturbation wavenumber l are identical to those cases shown in figure 1. Here, the dissipative NLS equation (3.11) is solved with $\lambda = 0.125$. In figure 3(a) and 3(b), the values of l lie in the instability range, and the initial behaviour shows a modulational instability despite viscous dissipation, in agreement with the analysis in the previous section for small λ. Compared to the corresponding cases in figure 1, the spikes are attenuated at later times for both the complex and the simple recurrence. In figure 3(c), the value $l = 4$ lies outside the instability range.

The norm for viscous gravity waves is plotted in figure 4. In figure 4(a), $\lambda = 0.125$ as in figure 3, and the dependence of the modulation on the perturbation wavenumber examined. The amplitudes of the recurrence are attenuated, as is also seen in figure 3, and the spikes are smoother. The value $l = 0.05$ lies within the instability range in the inviscid limit ($\lambda = 0$), but shows decay in figure 4(a). The effect of λ is illustrated in figure 4(b) with $l = 2$ fixed. As λ becomes larger, the amplitude and periodic of recurrence decrease; when $\lambda = 0.5$, we observe monotonic decay. Figure 4(c) shows the effect of the disturbance amplitude b when $l = 2$. For small time the growth rate does not demonstrate amplitude dependence, whereas for larger time the recurrence period increases as b decreases. Other calculations for neutral stability (e.g. $l = 4$) shows that the modulational behaviour is hardly affected by changes in b and is almost exclusively dependent on l, as expected from the linear analysis.

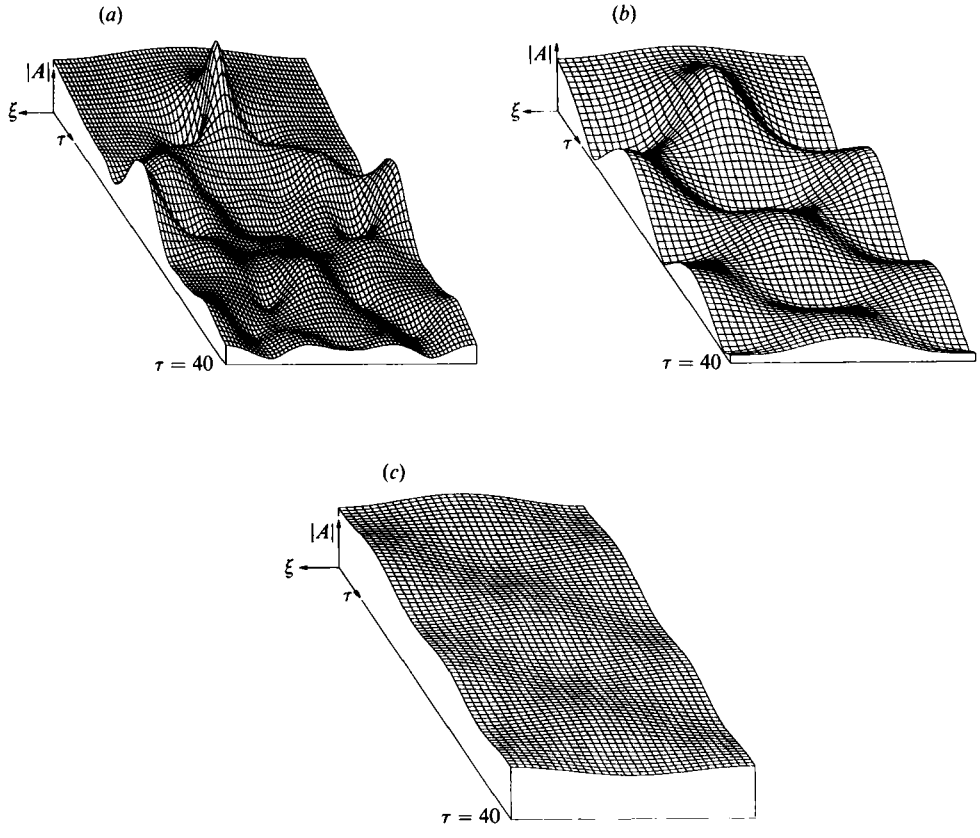

FIGURE 3. Evolution of modulations for gravity waves with small viscosity ($\lambda = 0.125$) in physical space $-2\pi/l < \xi < 0$: (*a*) $l = 1$; (*b*) $l = 2$; (*c*) $l = 4$.

For capillary–gravity waves with surfactants, the dissipative NLS equation is given by (4.15). The coefficient for the dissipation term is independent of the Weber number T_0, and the coefficients for the dispersion and nonlinear terms depend only on T_0. The term that corresponds to the frequency change in the coefficient for the dissipation term can be absorbed in the carrier wave and does not contribute to the magnitude of the envelope wave. The qualitative behaviour of the modulation is then expected to be identical to that for the gravity waves when T_0 is outside the range (5.3), for the so-called self-focusing type of NLS equation. When T_0 is in the range (5.3), equation (4.15) is of the defocusing type. Then, the long-time modulation exhibits quite different features from the simple oscillation with constant amplitude and frequency found for neutral stability of the self-focusing type. A discussion of self-focusing and defocusing NLS equations was given by Peregrine (1983).

Figure 5 shows the evolution of inviscid capillary–gravity waves ($\kappa = \lambda = 0$). The perturbation wavenumber is chosen as $l = 2$, and four different values of surface tension are considered. For pure gravity waves ($T_0 = 0$), the maximum growth rate and simple recurrence are observed as in figure 3. For pure capillary waves ($T_0 = 1$), $l = 2$ lies outside the instability region; thus, an oscillation is observed with constant amplitude and frequency. For $T_0 = 0.1$, $l = 2$ is closer to the lower bound of the instability region $l = 0$, and so complex recurrence occurs. The value $T_0 = 0.3$ lies between $1 - \sqrt{\frac{3}{2}}$ and $\frac{1}{3}$, and the modulation shows initial neutral stability, as predicted

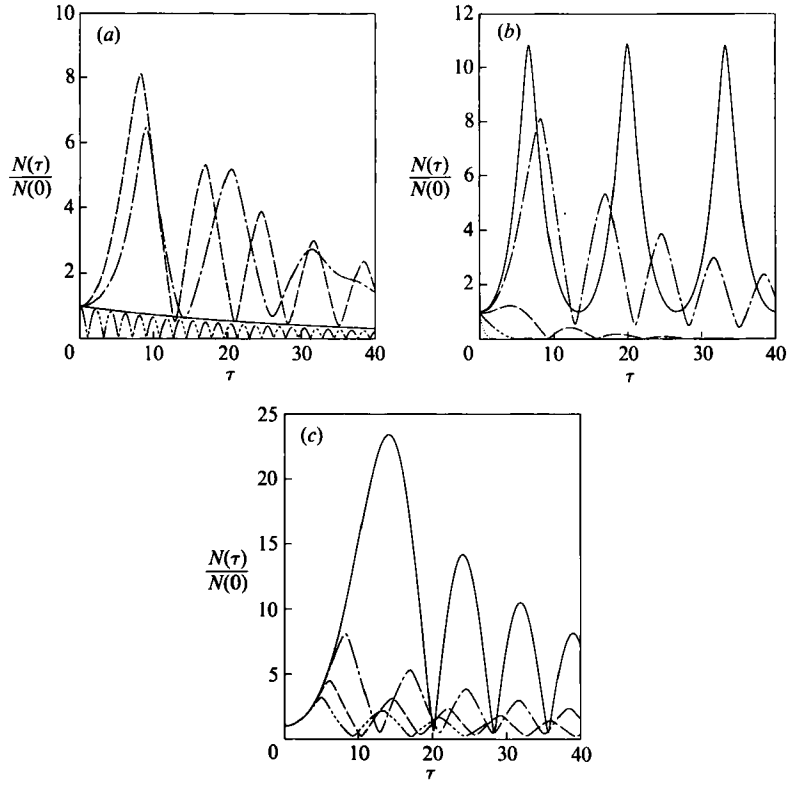

FIGURE 4. Evolution of modulations for gravity waves: (*a*) $\lambda = 0.125$ and $b = 0.1$ are fixed, and the perturbation wavenumber varies as $l = 0.05$ (——), $l = 1$ (— — —), $l = 2$ (– – –), and $l = 4$ (— · — · —); (*b*) $l = 2$ and $b = 0.1$ are fixed, and the viscous dissipation varies as $\lambda = 0$ (——), $\lambda = 0.125$ (— — —), $\lambda = 0.25$) (– – –), $\lambda = 0.5$ (— · — · —), and $\lambda = 1$ (.....); (*c*) $l = 2$ and $\lambda = 0.125$ are fixed, and the perturbation varies as $b = 0.01$ (——), $b = 0.1$ (— — —), $b = 0.2$ (– – –), and $b = 0.3$ (— · — · —).

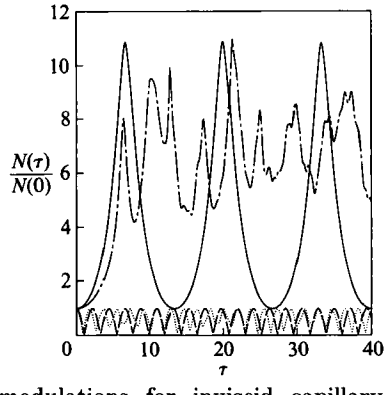

FIGURE 5. Evolution of modulations for inviscid capillary–gravity waves ($\lambda = \kappa = 0$) for perturbation wavenumber $l = 2$ and Weber number: T_0 (——), $T_0 = 0.1$ (— — —), $T_0 = 0.3$ (.....), and $T_0 = 1$ (– – –).

by the analysis. However, for large time an additional periodic behaviour is observed. The large-scale period increases as l decreases, as can be seen in figure 6 (*a*), where $l = 1$ while the other parameters remain unchanged ($T_0 = 0.3$ and $\kappa = \lambda = 0$). The corresponding profile for amplitude evolution is given in figure 6 (*b*). Initially, the

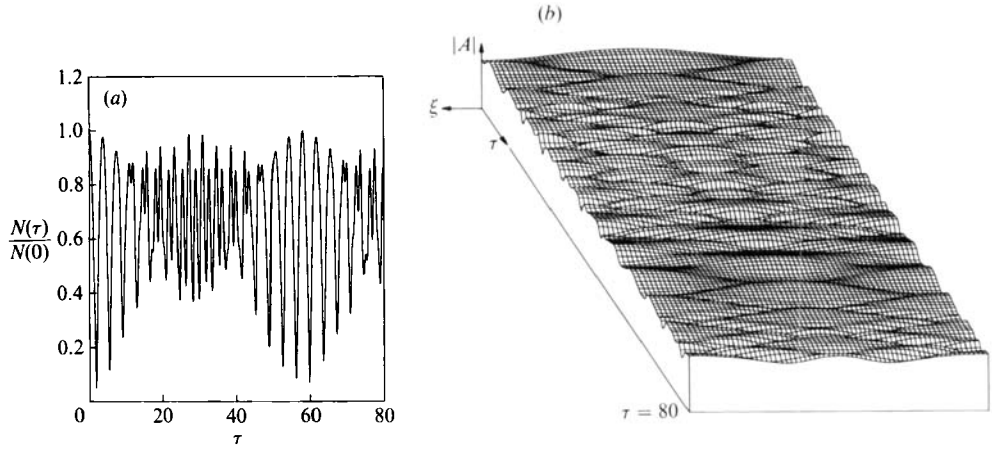

FIGURE 6. Evolution of modulations for inviscid capillary–gravity waves ($\lambda = \kappa = 0$) for perturbation wavenumber $l = 1$ and Weber number $T_0 = 0.3$: (*a*) $N(\tau)/N(0)$; (*b*) $|A(\xi, \tau)|$.

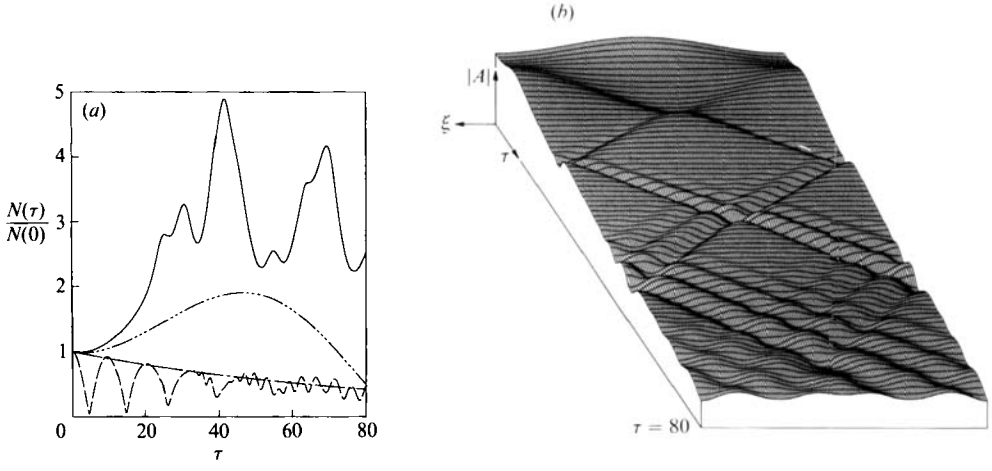

FIGURE 7. Evolution of modulations for capillary–gravity waves in the presence of viscosity ($\lambda = 0.125$) and surfactant ($\kappa = \sqrt{2}$) for perturbation wavenumber $l = 1/\sqrt{6}$ and Weber number: (*a*) $T_0 = 0.1$ (——), $T_0 = 0.1339$ (— — —), $T_0 = 0.3$ (– – –), and $T_0 = 1$ (— · · · —); (*b*) $T_0 = 0.3$, physical space $-2\pi/l < \xi < 0$.

behaviour is similar to that for neutral stability, but the amplitude then gradually decreases and the frequency starts to change until the initial envelope disintegrates at about $\tau = 30$; still later ($\tau \approx 60$), the initial form of the envelope is almost completely recovered. Therefore, this phenomenon can be referred to as a small-amplitude recurrence, different from the recurrence related to Benjamin–Feir instability.

In figure 7, we examine the effect of dissipation due to viscosity and a surfactant; $\lambda = 0.125$, $\kappa = \sqrt{2}$, and $l = 1/\sqrt{6}$. The perturbation wavenumber corresponds to the maximum growth rate for inviscid pure capillary waves. The norm for the case $T_0 = 1$ grows to a maximum at twice its initial value near $\tau = 50$ (figure 7*a*). When $T_0 = 0.1$, the instability with complex recurrence is observed despite viscous dissipation, whereas for T_0 slightly smaller than $1 - \sqrt{\frac{3}{2}}$ ($T_0 = 0.1339$), the complex recurrence is

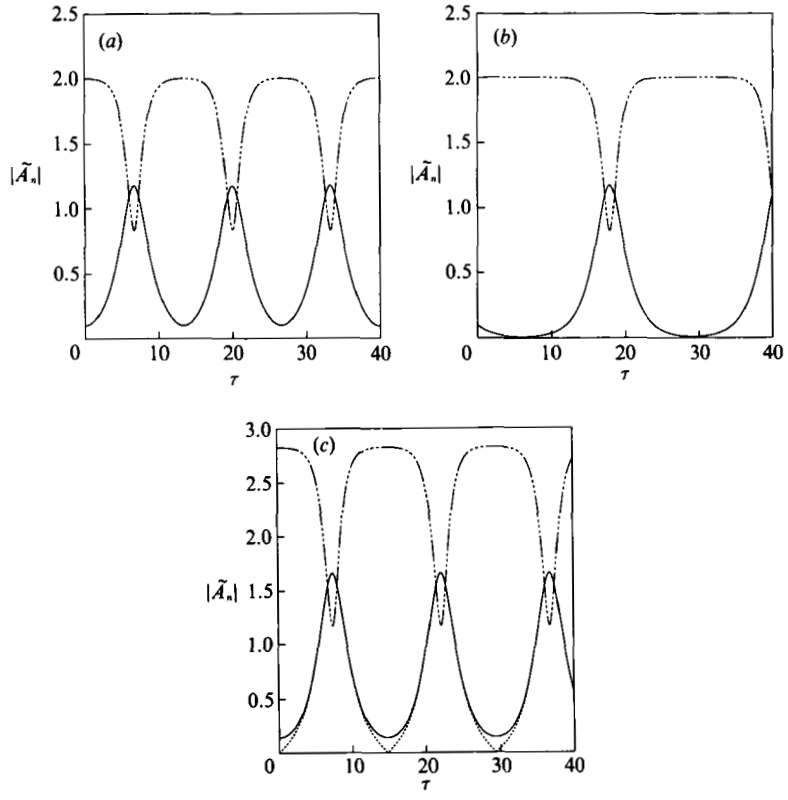

FIGURE 8. Evolution of dominant Fourier modes for inviscid gravity waves for $l = 2$ and initial sideband amplitudes: (*a*) $B_1 = B_2 = 0.05$ for $n = 0$ (– – –) and $n = \pm 1$ (——); (*b*) $B_1 = 0.05$ and $B_2 = 0.05\mathrm{i}$ for $n = 0$ (– – –) and $n = \pm 1$ (——); (*c*) $B_1 = 0.05$ and $B_2 = 0$ for $n = 0$ (– – –), $n = -1$ (——), and $n = 1$ (------).

suppressed by dissipation, and monotonic decay is observed. For $T_0 = 0.3$, a disintegration of the wave envelope is obvious even with viscous damping, as can be seen clearly in the corresponding evolution profile in figure 7(*b*). From figure 7, we can also deduce that the period of the disintegration-recovery has increased from that in figure 6 because a smaller l has been considered.

In all the calculations above, the initial condition used is (5.4), which corresponds to a symmetric amplitude modulation. We now consider more general modulations by using (5.1) instead, with $B_1(0)$ and $B_2(0)$ not necessarily equal and real as in (5.4). For simplicity, the results for inviscid gravity waves are presented in figure 8. Only the dominant fundamental and the sideband modes are plotted. In all the cases considered, the wavenumber perturbation is $l = 2$, so that all exhibit an initial Benjamin–Feir instability followed by simple recurrence. In figure 8(*a*), the given initial condition is identical to those in figure 1(*a*, *b*), and so the results are identical. In figure 8(*b*), it is obvious that the phase difference changes the modulational behaviour significantly, including the recurrence period. Figure 8(*c*) shows the effect of different initial sideband amplitudes, here showing an increase in the recurrence period with a decrease in amplitude. In figure 8(*c*), only one of the sideband modes is present initially, but subsequent evolution shows that the other mode is automatically excited to produce the Benjamin–Feir instability. The initially

different sideband amplitudes in figure 8(c) become nearly identical, as predicted by Stiassnie & Kroszynski (1982), but they recover their difference periodically in the subsequent recurrence.

6. Concluding remarks

The methods of multiple scales and matched asymptotic expansions have been used in a formal derivation of evolution equations for weakly nonlinear viscous water waves. The result is the nonlinear Schrödinger equation with an additional linear dissipation term. The present analysis is valid when both the amplitude of the wave and the viscous effect (or equivalently boundary-layer thickness) are small, and is restricted to wave packets with narrow-banded spectra. For both gravity waves and capillary–gravity waves with an insoluble surfactant, the largest terms in the damping coefficients are identical to classical linear results. For capillary–gravity waves, non-uniformities are observed despite dissipation due to the surfactant. Near the second-harmonic resonance, a modified state of evolution equations is obtained, which are matched asymptotically with the non-resonant results. For pure capillary waves, a rescaling of the long-scale free-surface elevation is required in the presence of surfactants.

The derived evolution equations are solved numerically to examine the modulation of infinite wavetrains with sideband disturbances of the Benjamin–Feir type. The computations show that in the presence of dissipation the modulation has the same initial behaviour as the inviscid case but eventually decays to zero in agreement with linear theory. In the inviscid limit, the instability condition obtained originally by Benjamin & Feir (1967) is recovered for gravity waves, whereas a stable range of Weber number is found for capillary–gravity waves, which agrees with that obtained by Djordjevic & Redekopp (1977). In this range, spectral computations show a new type of recurrence not directly related to the Benjamin–Feir instability.

One of the original goals of this study was to determine the validity of the linear dissipation terms added to the amplitude equations of previous studies. We found that the scaling restrictions required to obtain dissipation in the amplitude equation at third order do not allow nonlinear dissipation – a higher-order analysis would be required. Adding an insoluble surfactant with a linear dependence of surface-tension coefficient on concentration again allows only linear dissipation, consistent with many experimental observations. Soluble or diffusive surfactants generally exhibit smaller surface dilational modulus (Levich 1962), but we have determined that these modifications would also have dissipative terms that are predicted by linear theory. However, nonlinear dissipation may be modelled using a nonlinear or time-dependent surface-tension constitutive relationship. Since this type of relationship has not been experimentally documented, we leave this for further study.

The results for capillary–gravity waves near the second-harmonic resonance are unaffected by viscosity or surfactant because the amplitude of the wave is taken to be much larger than the boundary-layer thickness. If the two were taken to be of the same order, the coupled evolution equations would be modified by dissipative terms. The present method will allow us to examine the effect of dissipation or surfactants on Wilton's ripples.

This work was supported by the Program in Ship Hydrodynamics at The University of Michigan funded by the University Research Initiative of the Office of Naval Research Contract N000184-86-K-0684, ONR Ocean Engineering Contract

N00014-87-0509. The authors acknowledge Professor J. Boyd for his valuable references and help in computations.

REFERENCES

ADDISON, J. V. & SCHECHTER, R. S. 1979 An experimental study of the rheological behavior of surface films. *AIChE J.* **25**, 32–41.

BENJAMIN, T. B. & FEIR, J. E. 1967 The disintegration of wave trains on deep water. *J. Fluid Mech.* **27**, 417–430.

CRAIK, A. D. D. 1982 The drift velocity of water waves. *J. Fluid Mech.* **116**, 187–205.

DAVEY, A. & STEWARTSON, K. 1974 On three-dimensional packets of surface waves. *Proc. R. Soc. Lond.* A **338**, 101–110.

DIAS, F. & BRIDGES, T. J. 1990 The third-harmonic resonance for capillary-gravity waves with $O(2)$ spatial symmetry. *Stud. Appl. Maths* **82**, 13–35.

DJORDJEVIC, V. D. & REDEKOPP, L. G. 1977 On two-dimensional packets of capillary-gravity waves. *J. Fluid Mech.* **79**, 703–714.

DOERING, C. R., GIBBON, J. D., HOLM, D. D. & NICOLAENKO, B. 1988 Low-dimensional behavior in the complex Ginzburg–Landau equation. *Nonlinearity* **1**, 279–309.

FERMI, I. E., PASTA, J. & ULAM, S. 1965 Studies of nonlinear problems. In *Collected papers of Enrico Fermi*, vol. II. (ed. Segre, E.) Document LA-1940, p. 978. University of Chicago.

GOODRICH, F. C. 1960 The mathematical theory of capillarity I – III. *Proc. Roy. Soc. Lond.* A **260**, 481–509.

GOODRICH, F. C. 1962 On the damping of water waves by monomolecular films. *J. Phys. Chem.* **66**, 1858–1863.

HASIMOTO, H. & ONO, H. 1972 Non-linear modulation of gravity waves. *J. Phys. Soc. Japan* **33**, 805.

HENDERSON, D. M. & HAMMACK, J. L. 1987 Experiments on ripple instabilities. Part 1. Resonant triads. *J. Fluid Mech.* **184**, 15–41.

HOLMES, C. A. 1985 Bounded solutions of the nonlinear parabolic amplitude equations for plane Poiseuille flow. *Proc. R. Soc. Lond.* A **402**, 299–322.

JOO, S. W. 1989 A study of water waves with capillary effects. Ph.D. thesis, University of Michigan, Ann Arbor, Department of Mechanical Engineering and Applied Mechanics.

KAWAI, S. 1979 Generation of initial wavelets by instability of a coupled shear flow and their evolution to wind waves. *J. Fluid Mech.* **93**, 661–703.

KEEFE, L. 1985 Dynamics of perturbed wavetrain solutions to the Ginzburg–Landau equation. *Stud. Appl. Math.* **73**, 91–153.

KOPELL, N. & HOWARD, L. N. 1981 Target patterns and horseshoes from a perturbed central-force problem: Some temporally periodic solutions to reaction-diffusion equations. *Stud. Appl. Maths* **64**, 1–56.

LAKE, B. M., YUEN, H. C., RUNGALDIER, H. & FERGUSON, W. E. 1977 Nonlinear deep-water waves: theory and experiment. Part 2. Evolution of a continuous wave train. *J. Fluid Mech.* **83**, 49–74.

LAMB, H. 1932 *Hydrodynamics*, 6th edn. Cambridge University Press.

LEVICH, V. G. 1941 *Zh. Eksp. Theor. Fiz.* **11**, 340.

LEVICH, V. G. 1962 *Physicochemical Hydrodynamics*. Prentice-Hall.

LIU, A.-K. & DAVIS, S. H. 1977 Viscous attenuation of mean drift in water waves. *J. Fluid Mech.* **81**, 63–84.

LUCASSEN, J. 1982 Effect of surface-active material on the damping of gravity waves: a reappraisal. *J. Colloid Interface Sci.* **85**, 52–58.

LUCASSEN-REYNDERS, E. H. & LUCASSEN, J. 1969 Properties of capillary waves. *Adv. Colloid Interface Sci.* **2**, 347–395.

LONGUET-HIGGINS, M. S. 1953 Mass transport in water waves. *Phil. Trans. R. Soc. Lond.* A **245**, 535–581.

McGoldrick, L. F. 1970 On Wilton's ripples: a special case of resonant interactions. *J. Fluid Mech.* **42**, 193–200.

Mei, C. C. 1983 *The Applied Dynamics of Ocean Surface Waves.* Wiley.

Miles, J. W. 1967 Surface wave damping in closed basins. *Proc. R. Soc. Lond.* A **297**, 459–475.

Miles, J. W. 1988 The evolution of a weakly nonlinear, weakly damped, capillary–gravity wave packet. *J. Fluid Mech.* **187**, 141–154.

Newell, A. C. & Whitehead, J. A. 1969 Finite bandwidth, finite amplitude convection. *J. Fluid Mech.* **38**, 279–303.

Peregrine, D. H. 1983 Water waves, nonlinear Schrödinger equations and their solutions. *J. Austral. Math. Soc.* B **25**, 16–43.

Pereira, N. R. & Stenflo, L. 1977 Nonlinear Schrödinger equation including growth and damping. *Phys. Fluids* **20**, 1733–1734.

Phillips, O. M. 1966 *Dynamics of the Upper Ocean.* Cambridge University Press.

Pliny, 77 AD *Naturalis Historia*, Book ii, Chap. 107, §234.

Reynolds, O. 1880 On the effect of oil on destroying waves on the surface of water. *Br. Assoc. Rept.*; *Papers* **1**, 409.

Stewartson, K. & Stuart, J. T. 1971 A non-linear instability theory for a wave system in plane Poiseuille flow. *J. Fluid Mech.* **48**, 529–545.

Stiassnie, M. & Kroszynski, U. I. 1982 Long-time evolution of an unstable water–wave train. *J. Fluid Mech.* **116**, 207–225.

Stokes, G. G. 1845 On the theories of the internal friction of fluids in motion. *Trans. Camb. Phil. Soc.* **8**, 287.

Stuart, J. T. & DiPrima, R. C. 1978 The Eckhaus and Benjamin–Feir resonance mechanisms. *Proc. R. Soc. Lond.* A **362**, 27–41.

Tempel, M. van den & Riet, R. P. van de 1965 Damping of waves by surface-active material. *J. Chem. Phys.* **42**, 2769–2777.

Ünlüata, U. & Mei, C. C. 1970 Mass transport in water waves. *J. Geophys. Res.* **75**, 7611–7618.

Weideman, J. A. C. & Herbst, B. M. 1987 Recurrence in semidiscrete approximations of the nonlinear Schröinger equation. *SIAM J. Sci. Stat. Comput.* **8**, 988–1004.

Yuen, H. C. & Ferguson, W. E. 1978 Relationship between Benjamin–Feir instability and recurrence in the nonlinear Schrödinger equation. *Phys. Fluids* **21**, 1275–1278.

Yuen, H. C. & Lake, B. M. 1980 Instabilities of waves in deep water. *Ann. Rev. Fluid Mech.* **12**, 303–334.

Yuen, H. C. & Lake, B. M. 1982 Nonlinear dynamics of deep-water gravity waves. *Adv. Appl. Mech.* **22**, 67–229.

Zakharov, V. E. 1968 Stability of periodic waves of finite-amplitude on the surface of deep fluid. *J. Appl. Mech. Tech. Phys.* **9**, 190–194.